Matters arising

On the robustness of topological gap detection via transport

https://doi.org/10.1038/s41586-026-10567-8

Received: 27 March 2025

Accepted: 20 April 2026

Check for updates

Henry F. Legg[1,2]✉

ARISING FROM: Microsoft Azure Quantum. *Nature* https://doi.org/10.1038/s41586-024-08445-2 (2025).

The detection of a topological superconducting phase—the basis of proposed topological qubits—is notoriously difficult because trivial states can mimic the signatures expected from a topological superconductor[1–6]. Microsoft Azure Quantum[7] reported single-shot parity readout of devices that are purportedly tuned into a topological superconducting phase using their transport-based tune-up procedure known as the topological gap protocol (TGP)[8]. Here, however, I analyse the underlying transport data—which were not presented in ref. 7—and this analysis reveals that the claimed parity readout occurred in regions of phase space with considerable disorder that appear gapless. The absence of a robust superconducting gap would contradict the prerequisite for the interpretation in ref. 7, suggesting instead that the observed signals arise from trivial mechanisms.

I focus here on the transport data used to establish the existence of a (topological) superconducting gap, rather than directly assessing the random telegraph signal in quantum capacitance interpreted as parity readout in ref. 7. However, such an interpretation necessitates the presence of a superconducting gap to protect the nanowire from low-energy quasiparticles. To establish this prerequisite, ref. 7 uses the TGP to select key device parameters—such as parallel magnetic field strength and gate voltage—where the claimed parity readout occurs. As such, the transport data underlying the TGP are central to all measurements and claims reported in ref. 7.

It was recently[9] shown that the TGP can be sensitive to the choice of data parameters, such as the cutter pair (controlling junction transparency), magnetic field range and bias voltage range. Furthermore, although only gapped outcomes were presented in ref. 7, I find that the TGP can also classify regions of purported parity readout as gapless. For example, in device A2, only the gapped outcome from cutter 1 was presented; however, the TGP applied to cutter 2 declares this same region as gapless. Further analysis of TGP parameter sensitivities is provided in Supplementary Note 1.

In addition to the TGP's inherent sensitivity to data parameters, the specific implementation of the TGP in ref. 7 contained coding artefacts that led to the omission of supposed topological regions. Specifically, in ref. 7, per device, the claimed parity readout was reported for only a single magnetic field value within a single region identified by the TGP. The omission of other TGP-passing regions stemmed from two coding artefacts: (1) the TGP plotting code was set to highlight only the largest purportedly topological region; and (2) the code antisymmetrized bias voltage based on array index rather than physical value. This latter issue introduced errors because the experimental bias data in ref. 7 are not symmetric around zero (for example, in device A1, bias voltages run from −66.18 μV to +63.64 μV). Correcting these coding artefacts reveals additional supposed topological regions (Fig. 1b) that were not explored. Notably, these corrections reveal that the capacitance measurements for device B in ref. 7 focused on a small, secondary region (Fig. 1, vertical dashed line) rather than the primary region(s) identified by the TGP. Finally, Fig. 1 further highlights the fragility of the TGP, demonstrating how even a single bias voltage datapoint can determine whether a region is classified as topological.

Random telegraph signals are ubiquitous in mesoscopic systems, such as quantum dots[10–12]. To rule out trivial origins it was therefore important for the authors of ref. 7 to test their interpretation elsewhere in phase space. When a reviewer asked "Are there other regions where things didn't work out?", the authors stated that, in each device, that they had investigated the "only region passing the TGP within the explored gate voltage and magnetic field range". However, this statement was inaccurate: other TGP-passing regions existed in phase space but were not explored in ref. 7. As such, the coding artefacts above leave the main claim in ref. 7 lacking a critical validation (or falsification) step that was requested by the reviewers.

The inconsistent (and incorrect) TGP outcomes highlight the problems with using the TGP as a diagnostic tool for a (topological) superconducting gap. Given these issues, I instead investigate the raw local and nonlocal conductance underlying the TGP outcomes. I focus here on device A2, although similar features are observed across all devices (Extended Data Figs. 1 and 2). It should be emphasized that no raw transport data were presented in ref. 7 (or its supplementary information), only TGP classification maps.

First, local conductance measurements reveal a significant number of low-energy states. For example, device A2 (cutter 2) displays strong finite conductance across the full bias range and has considerable structure (Fig. 2j,m). This seemingly indicates an abundance of low-energy states as, if the device was in the Andreev enhanced regime, that would contradict the tunnelling regime in which the TGP was defined[8]. Similarly, the zero-bias peak for cutter 1 on the left fills almost the entire bias range (Fig. 2n) and has considerable structure. By contrast, the zero-bias peak is barely visible on the right (Fig. 2m). Similar evidence of disorder and poorly defined zero-bias peaks is observed across all devices in ref. 7 (Extended Data Figs. 1 and 2). Finally, I note that there is often a sizeable difference in the magnitude of the local conductance on each side of the nanowire, indicating highly asymmetric tunnel barriers; no justification is provided in ref. 7 for this.

The nonlocal conductance (Fig. 2k,l) also reveals a complex signal, often with conductance throughout the bias range. This appears consistent with a gapless system, as indicated by some TGP outcomes (for example, cutter 2 of device A2). Note that the TGP's antisymmetrization in bias voltage renders it blind to symmetric nonlocal conductance. This means that a topological gap can be reported by the TGP (indicated by dashed lines in conductance plots), despite significant nonlocal conductance at low bias.

[1]SUPA, School of Physics and Astronomy, University of St Andrews, St Andrews, UK. [2]Department of Physics, University of Basel, Basel, Switzerland. ✉e-mail: hl29@st-andrews.ac.uk

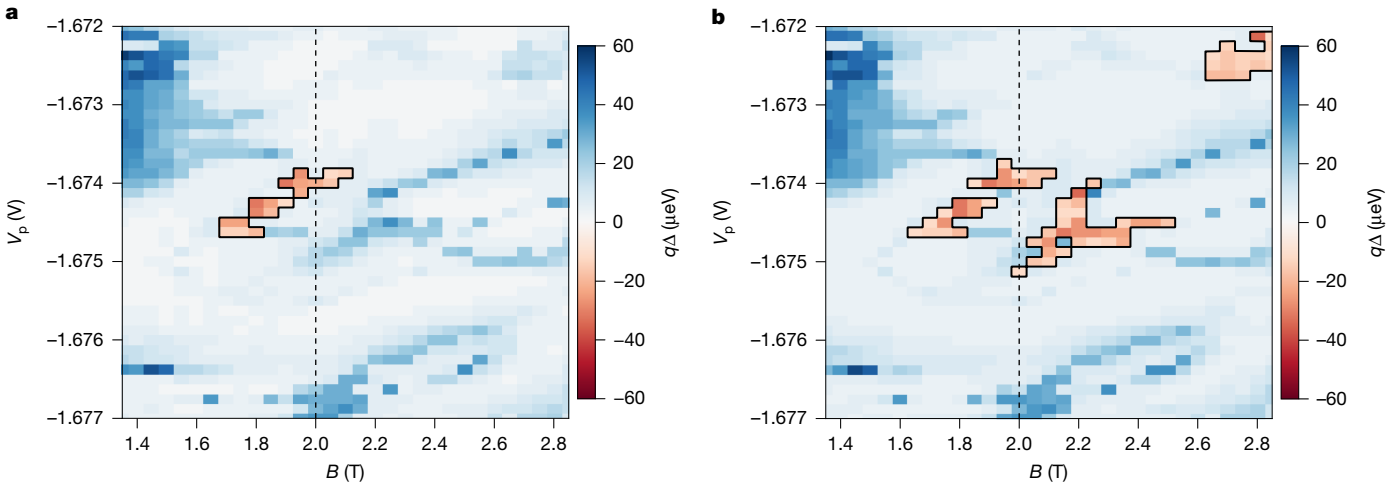

Fig. 1 | Impact of coding artefacts on transport based topological gap detection. a, The outcome of the TGP reported in ref. 7. The red regions indicate topological classification by the TGP. The vertical dashed line shows the single magnetic field value (B = 2.0 T) where parity readout purportedly occurred. **b**, The TGP outcome for device B after correcting coding artefacts (that is, now flagging all identified regions and removing the one bias value that caused the range to be asymmetric). This corrected TGP outcome reports multiple regions of phase space as topological. Note that, after correction, the magnetic field value used for the purported parity readout corresponds to a secondary region. The larger regions were not explored in ref. 7 even though, if the author's interpretations were correct, parity readout should have been possible here too. This figure also highlights the TGP's sensitivity to data parameters, because the significant changes in **b** result from removing a single bias voltage—a parameter that is not visible in these plots.

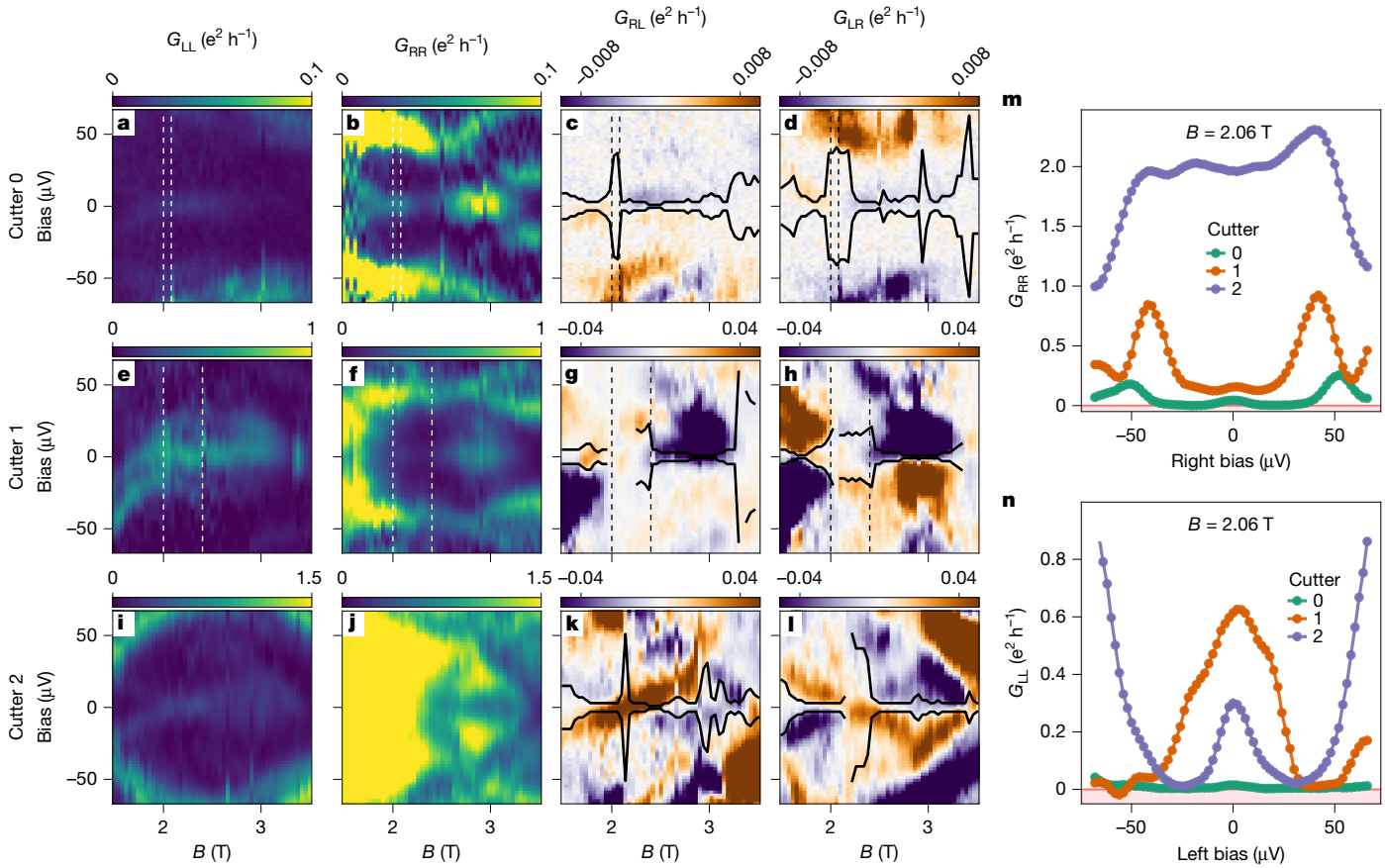

Fig. 2 | Transport data underlying the TGP tune-up of device A2. **a**–**n**, Conductance matrix (local conductance G_{LL} (**a**,**e**,**i**) and G_{RR} (**b**,**f**,**j**), as well as nonlocal conductance G_{RL} (**c**,**g**,**k**) and G_{LR} (**d**,**h**,**l**)) for three junction settings (cutters 0 (**a**–**d**), 1 (**e**–**h**) and 2 (**i**–**l**)) in the supposed topological region (**a**–**l**) and conductance line cuts at the purported readout field (G_{RR} (**m**) and G_{LL} (**n**)). Note the varying scales on colour bars and y axes due to significant variations in size of conductance for the TGP tune-up data in this case. These conductance data appear to show an abundance of low-energy states, for example, cutter 2 (**i**–**l**) and the purple trace in **m** show substantial low-energy conductance, with considerable structure, rising above even 2 e^2 h^{-1}. The black lines indicate the gap extracted by the TGP. Note that the TGP can classify the system as gapped despite significant low-bias nonlocal conductance (**k**,**l**) because the TGP's antisymmetrization in bias ignores symmetric contributions to nonlocal conductance. Parameters: V_p = −1.8444 V, B = 2.06 T.

Finally, the authors of ref. 7 stated to the referees that they had not detected the formation of accidental quantum dots, "as such dots would typically induce particle-hole symmetry breaking". However, the underlying conductance data contradict this assertion. For a gapped system, the local conductance is expected to be symmetric around zero bias[13], yet the data often exhibit considerable low-bias asymmetry, for example, for cutter 1 on the left (Fig. 2n). More generally, three-terminal devices with particle-hole symmetry are expected to obey relations between local and nonlocal conductance[14], but these relationships do not hold for the regions studied in ref. 7 (Supplementary Note 2). Furthermore, there are regions of (asymmetric) negative local conductance, a signature associated with the presence of quantum dots[3,14,15] (Supplementary Note 2).

In summary, my analysis highlights key issues with the transport data underpinning the main claim of ref. 7. The tune-up method used to identify a gapped (topological) superconducting phase—the TGP—yielded inconsistent and misreported outcomes. Furthermore, the underlying transport data, which were not presented in ref. 7, reveal an apparent abundance of low-energy states, signatures of quantum dots and no clear (topological) superconducting gap. The absence of a robust superconducting gap contradicts the prerequisite needed to interpret the observed random telegraph signal as a parity measurement. I also note that using the interpreted capacitance signal to retrospectively establish the existence of a (topological) SC gap reverses the hierarchy of evidence presented in the original paper. Consequently, I conclude that the transport data underpinning ref. 7 strongly suggest that alternative, non-topological explanations, such as quantum dot physics, should be considered as the origins for the measurements reported in ref. 7.

Data availability

No new data were generated in this study. The transport data for the original study are available at Zenodo[16] (https://doi.org/10.5281/zenodo.14804380).

Code availability

The code to reproduce the figures is available at Zenodo[17] (https://doi.org/10.5281/zenodo.15008728).

1. Rainis, D., Trifunovic, L., Klinovaja, J. & Loss, D. Towards a realistic transport modeling in a superconducting nanowire with Majorana fermions. *Phys. Rev. B* **87**, 024515 (2012).
2. Kells, G., Meidan, D. & Brouwer, P. W. Near-zero-energy end states in topologically trivial spin-orbit coupled superconducting nanowires with a smooth confinement. *Phys. Rev. B* **86**, 100503 (2012).
3. Lee, E. J. H. et al. Zero-bias anomaly in a nanowire quantum dot coupled to superconductors. *Phys. Rev. Lett.* **109**, 186802 (2012).
4. Vuik, A., Nijholt, B., Akhmerov, A. R. & Wimmer, M. Reproducing topological properties with quasi-Majorana states. *SciPost Phys.* **7**, 061 (2019).
5. Prada, E. et al. From Andreev to Majorana bound states in hybrid superconductor–semiconductor nanowires. *Nat. Rev. Phys.* **2**, 575–594 (2020).
6. Hess, R., Legg, H. F., Loss, D. & Klinovaja, J. Trivial Andreev band mimicking topological bulk gap reopening in the nonlocal conductance of long Rashba nanowires. *Phys. Rev. Lett.* **130**, 207001 (2023).
7. Microsoft Azure Quantum. Interferometric single-shot parity measurement in InAs–Al hybrid devices. *Nature* **638**, 651–655 (2025).
8. Aghaee, M. et al. InAs-Al hybrid devices passing the topological gap protocol. *Phys. Rev. B* **107**, 245423 (2023).
9. Legg, H. F. Comment on "InAs-Al hybrid devices passing the topological gap protocol", Microsoft Quantum, *Phys. Rev. B* **107**, 245423 (2023). Preprint at *arXiv* https://doi.org/10.48550/arXiv.2502.19560 (2025).
10. Paladino, E., Galperin, Y. M., Falci, G. & Altshuler, B. L. 1/f noise: implications for solid-state quantum information. *Rev. Mod. Phys.* **86**, 361 (2014).
11. Bargerbos, A. et al. Singlet-doublet transitions of a quantum dot in a magnetic field. *PRX Quantum* **3**, 030311 (2022).
12. van Loo, N. et al. Single-shot parity readout of a minimal Kitaev chain. *Nature* **650**, 334–339 (2026).
13. Danon, J. et al. Nonlocal conductance spectroscopy of Andreev bound states: Symmetry relations and BCS charges. *Phys. Rev. Lett.* **124**, 036801 (2020).
14. Higginbotham, A. et al. Parity lifetime of bound states in a proximitized semiconductor nanowire. *Nat. Phys.* **11**, 1017–1021 (2015).
15. Fransson, J. & Eriksson, O. Current-voltage asymmetries and negative differential conductance due to strong electron correlations in double quantum dots. *Phys. Rev. B* **70**, 085301 (2004).
16. Microsoft (United States). Interferometric single-shot parity measurement in InAs-Al hybrid devices. *Zenodo* https://doi.org/10.5281/zenodo.14804379 (2025).
17. Legg, H. F. Comment on "Interferometric single-shot parity measurement in InAs–Al hybrid devices", Microsoft Quantum, *Nature* **638**, 651–655 (2025). *Zenodo* https://doi.org/10.5281/zenodo.15008728 (2025).

Acknowledgements I thank C. Dickel, S. Frolov, R. Hess, J. Klinovaja, L. Kouwenhoven, D. Loss, G. Mazur and V. Mourik for scientific discussions. I acknowledge previous discussions regarding the TGP with R. Lutchyn, C. Nayak and G. Winkler.

Author contributions H.F.L. performed the analysis and wrote the manuscript.

Competing interests The author declares no competing interests.

Additional information
Supplementary information The online version contains supplementary material available at https://doi.org/10.1038/s41586-026-10567-8.

Correspondence and requests for materials should be addressed to Henry F. Legg.

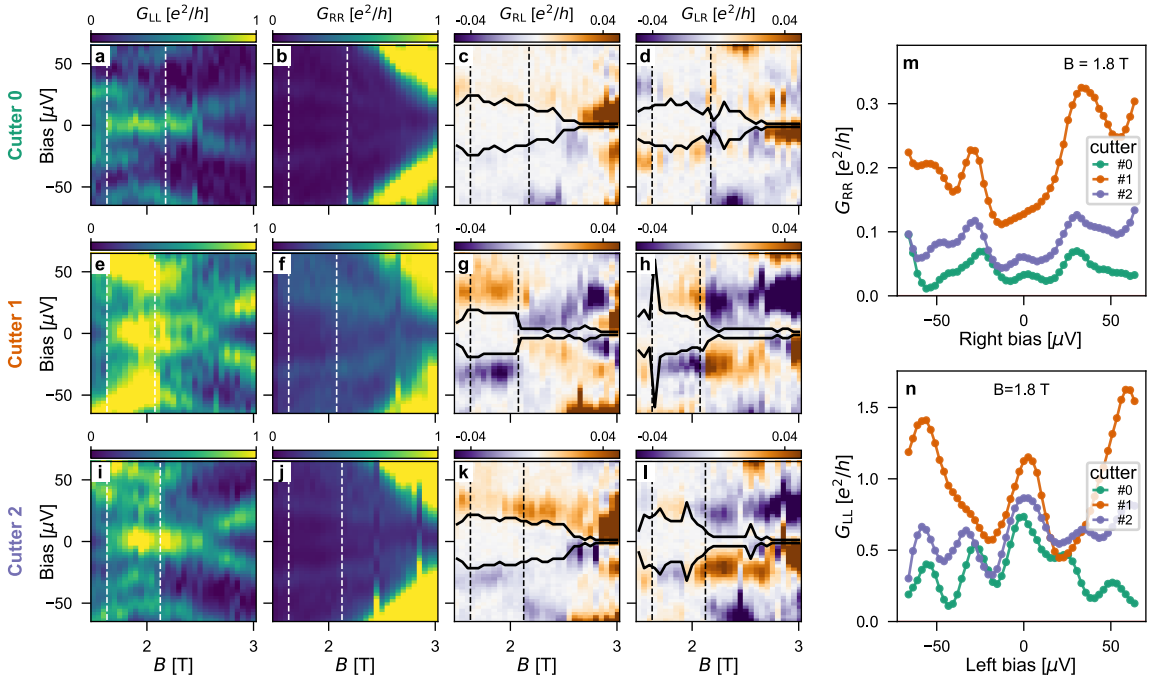

Extended Data Fig. 1 | Transport data underlying the TGP tune-up of Device A1. Conductance matrix for three junction settings (cutters 0–2) in the supposed topological region (a–l) and conductance line cuts at the purported readout field (m–n). The line cuts of local conductance on both sides of the device reveal a complex signal with considerable structure, suggesting the presence of multiple overlapping low-energy states. Parameters: $V_p = -1.82225$ V, B = 1.8 T.

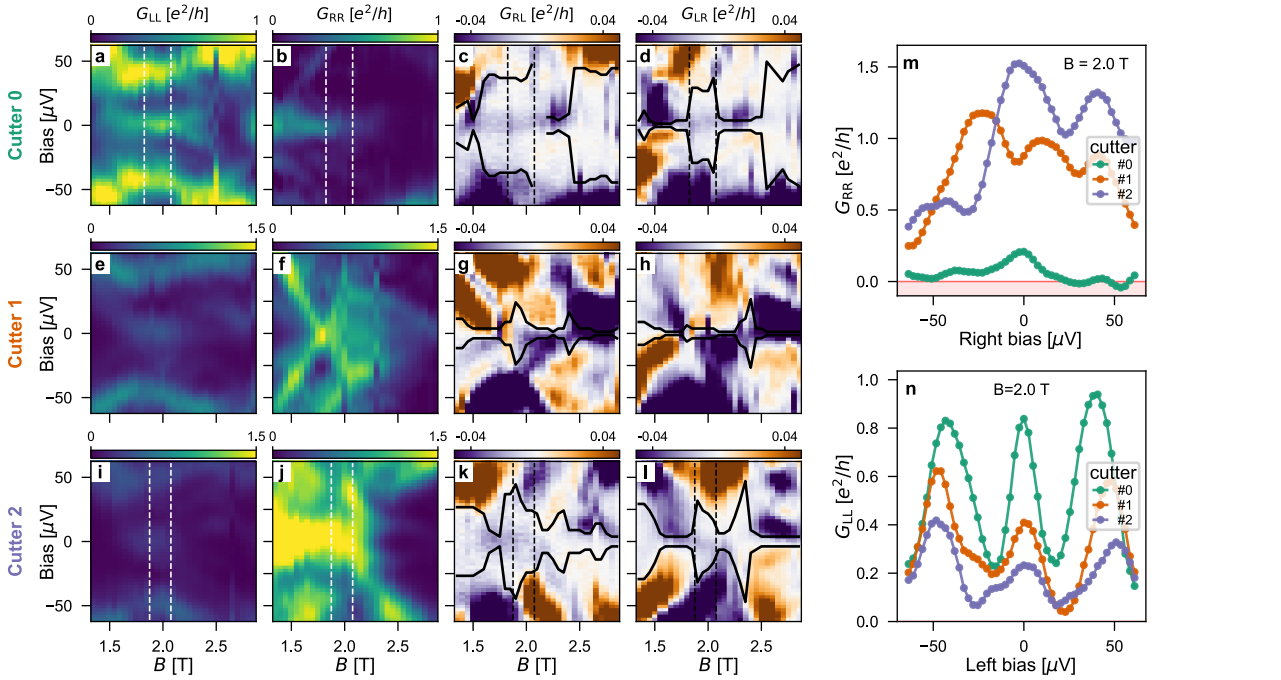

Extended Data Fig. 2 | Transport data underlying the TGP tune-up of Device B. Conductance matrix for three junction settings (cutters 0–2) in the supposed topological region (a–l) and conductance line cuts at the purported readout field (m–n). The line cuts reveal a complex signal with considerable structure in the local conductance on both sides of the device, suggesting the presence of multiple overlapping low-energy states. Additionally, cutter 0 exhibits substantial negative local conductance on the right side, a known signature of quantum dots (Supplementary Note 2). Parameters: $V_p = -1.6740$ V, B = 2.0 T.

Reply to: On the robustness of topological gap detection via transport

https://doi.org/10.1038/s41586-026-10568-7

Microsoft Quantum*

REPLYING TO: H. F. Legg. *Nature* https://doi.org/10.1038/s41586-026-10567-8 (2026).

In our previous study[1], we reported single-shot parity readout in an InAs–Al hybrid nanowire device, evidenced by an $h/2e$-flux-periodic random telegraph signal (RTS) in the quantum capacitance (C_Q). These radio frequency (RF) interferometric measurements strongly indicate a topological origin: they are consistent with our theoretical model and very strongly constrain non-topological explanations. In the accompanying Comment[2], Legg claimed that our transport data points to a gapless state. However, our analysis of our C_Q measurements does not assume the existence of a gap. Indeed, a gapless system would not exhibit a stable $h/2e$-periodic bimodal signal: the interferometric contrast would wash out due to collapse of the oscillation amplitude or time scales.

As shown in supplementary figure 4 and in the simulations of ref. 3, gap closure causes the bimodality of the capacitance signal to collapse: when multiple states approach zero energy, their contributions acquire random phases that suppress C_Q oscillations. Moreover, a gapless system should be indifferent to an additional quasiparticle, in contrast to our device, which shows a prominent quasiparticle-poisoning-induced telegraph signal (tested explicitly by injecting quasiparticles; supplementary information 7.3 of ref. 1). Our observed $\Delta C_Q \approx 1$ fF directly indicates operation in a region with a well-developed bulk energy gap, rendering the reasoning of Legg[2] regarding the tune-up procedure both irrelevant and untenable.

The topological gap protocol (TGP) served solely as a practical tuning tool to identify operating points; it had no role in interpreting the RF measurements that form the basis of our conclusions. Legg[2] interprets these transport data as pointing to a gapless state. However, as we review in more detail below, our TGP measurements are in fact consistent with a gapped state. This is why they are useful as a device tuning procedure. In combination, the RF and transport measurements in our original study[1] constitute very strong evidence that we have a gapped system exhibiting Majorana-mediated parity flips and very strongly constrain all known alternative scenarios.

While Legg[2] does not contest our RF capacitance observations or their quantitative agreement with our theoretical model, it asserts that our nanowire lacked a well-developed superconducting gap, based on an analysis of the raw three-terminal conductance data. Legg[2] highlights (1) substantial subgap conductance; (2) symmetric components in the nonlocal conductance; and (3) asymmetries and occasional negative differential conductance. Finite local conductance within the gap does not imply a gapless density of states. Our devices are operated in an intermediate junction transparency regime for sensitivity reasons. In this regime, a discrete subgap state can occasionally produce broad conductance features through Andreev enhancement. Thus, broad low-bias conductance does not prove a continuum of states; it probably reflects broadened discrete modes. Indeed, when the barriers were more pinched off, the resulting spectra had less sub-gap conductance, but at the cost of smaller signal amplitude. Sizeable symmetric components of the nonlocal conductance likewise do not indicate a gapless bulk. The transport gap cannot be reliably inferred from visual inspection alone and must be extracted by quantitative analysis; our procedure focused on the antisymmetric nonlocal conductance to minimize susceptibility to measurement-circuit non-idealities. A symmetric nonlocal component is not by itself evidence of gaplessness: such components are compatible with particle-hole symmetry in three-terminal devices and have been discussed extensively in the literature[4,5]. However, the symmetry relationships described in ref. 4 are derived under idealized assumptions that need not hold in experimental settings. For example, bias-dependent local matrix elements, such as those appearing in equation 1 of ref. 5, can naturally generate a symmetric component of the nonlocal conductance. However, Legg[2] does not pursue such an analysis and instead selectively emphasizes a quantum-dot-based interpretation of the data. Negative differential conductance is invoked as support for this idea, but physically only implies an energy dependence of the transmission probability; quantum-dot formation is one possible mechanism, but it is far from unique. Legg[2] neither provides nor attempts a self-consistent alternative interpretation of the full dataset, but instead points to generic complications.

As Legg[2] mentions the TGP's dependence on parameter values, we reiterate that the TGP is probabilistic and has a well-bounded but finite rate of false positives, as any such protocol should. One can change the thresholds that define the TGP, thereby changing TGP outcomes, for example, to reduce the rate of false positives but at the cost of increasing the number of false negatives. We have picked threshold values that give a false-positive rate that is low enough so that the TGP is a useful tune-up procedure for the parity measurement.

We now turn to aspects not addressed in our previous publications. Legg[2] identified a minor off-by-one-pixel bug in our TGP processing. The correction shifts extracted gap values by less than 5 μeV for more than 96% of pixels and introduces one new subregion of interest in device B. We have uploaded corrected TGP maps and a per-pixel delta map to Zenodo[6]; no changes to the parity-readout data or analysis are involved. The region used for parity readout remains classified as gapped after the fix. Other TGP-passing regions outside the explored parity-measurement range are fully consistent with our referee statement that "this was the only region passing the TGP within the explored range".

In our original study[1], our focus was on the flux-dependent RTS signal rather than an exhaustive phase-diagram mapping; performing parity measurements in every TGP-flagged region was outside the scope of the work. To demonstrate robustness, we repeated the experiment in the same device and on a second device, all showing flux-periodic RTS. We also showed that the $h/2e$ bimodal signal disappears when

*A list of authors and their affiliations appears at the end of the paper.

sweeping the wire-plunger voltage, going to low fields, cutting the interference loop or injecting quasiparticles, confirming that it is neither ubiquitous nor attributable to generic mesoscopic RTS mechanisms. Legg[2] does not engage with these checks or provide a consistent alternative model.

In summary, Legg[2] centres on a selective examination of transport tune-up procedures and narrow interpretations of isolated phrases in our referee correspondence, rather than the physical mechanisms underlying the experiment. It relies on unsubstantiated claims about our transport spectra while not engaging with the capacitance measurements at the core of our study, and its alternative treatment of the transport data is inconsistent with more rigorous analyses of the same datasets. Critically, Legg[2] offers no alternative physical model capable of reproducing the capacitance signal or the RTS phenomenology, and does not constitute a substantial scientific challenge to our findings.

Data availability

Corrected TGP maps and a per-pixel delta map are available at Zenodo[6] (https://doi.org/10.5281/zenodo.14804379).

1. Microsoft Azure Quantum. Interferometric single-shot parity measurement in InAs–Al hybrid devices. *Nature* **638**, 651–655 (2025).
2. Legg, H. F. On the robustness of topological gap detection via transport. *Nature* https://doi.org/10.1038/s41586-026-10567-8 (2026).
3. Boutin, S. et al. Predictive simulations of the dynamical response of mesoscopic devices. Preprint at *arXiv* https://doi.org/10.48550/arXiv.2502.12960 (2025).
4. Danon, J. et al. Nonlocal conductance spectroscopy of Andreev bound states: symmetry relations and BCS charges. *Phys. Rev. Lett.* **124**, 036801 (2020).
5. Kurilovich, V. D., Cole, W. S., Lutchyn, R. M. & Glazman, L. I. Nonlocal conductance of a majorana wire near the topological transition. Preprint at *arXiv* https://doi.org/10.48550/arXiv.2409.09325 (2024).
6. Microsoft (United States). Interferometric single-shot parity measurement in InAs-Al hybrid devices. *Zenodo* https://doi.org/10.5281/zenodo.14804379 (2025).

Author contributions The Microsoft Quantum team conceived and implemented the technology that is the basis for this article.

Competing interests The authors declare no competing interests.

Additional information
Correspondence and requests for materials should be addressed to Chetan Nayak.
Reprints and permissions information is available at http://www.nature.com/reprints.
Publisher's note Springer Nature remains neutral with regard to jurisdictional claims in published maps and institutional affiliations.

Microsoft Quantum

Morteza Aghaee[1], Alejandro Alcaraz Ramirez[1], Zulfi Alam[1], Rizwan Ali[1], Mariusz Andrzejczuk[1], Andrey Antipov[1], Mikhail Astafev[1], Amin Barzegar[1], Bela Bauer[1], Jonathan Becker[1], Umesh Kumar Bhaskar[1], Alex Bocharov[1], Srini Boddapati[1], David Bohn[1], Jouri Bommer[1], Leo Bourdet[1], Arnaud Bousquet[1], Samuel Boutin[1], Lucas Casparis[1], Benjamin J. Chapman[1], Sohail Chatoor[1], Anna Wulff Christensen[1], Cassandra Chua[1], Patrick Codd[1], William Cole[1], Paul Cooper[1], Fabiano Corsetti[1], Ajuan Cui[1], Paolo Dalpasso[1], Juan Pablo Dehollain[1], Gijs de Lange[1], Michiel de Moor[1], Andreas Ekefjärd[1], Tareq El Dandachi[1], Juan Carlos Estrada Saldaña[1], Saeed Fallahi[1], Luca Galletti[1], Geoff Gardner[1], Deshan Govender[1], Flavio Griggio[1], Ruben Grigoryan[1], Sebastian Grijalva[1], Sergei Gronin[1], Jan Gukelberger[1], Marzie Hamdast[1], Firas Hamze[1], Esben Bork Hansen[1], Sebastian Heedt[1], Zahra Heidarnia[1], Jesús Herranz Zamorano[1], Samantha Ho[1], Laurens Holgaard[1], John Hornibrook[1], Jinnapat Indrapiromkul[1], Henrik Ingerslev[1], Lovro Ivancevic[1], Thomas Jensen[1], Jaspreet Jhoja[1], Jeffrey Jones[1], Konstantin V. Kalashnikov[1], Ray Kallaher[1], Rachpon Kalra[1], Farhad Karimi[1], Torsten Karzig[1], Evelyn King[1], Maren Elisabeth Kloster[1], Christina Knapp[1], Dariusz Kocon[1], Jonne V. Koski[1], Pasi Kostamo[1], Mahesh Kumar[1], Tom Laeven[1], Thorvald Larsen[1], Jason Lee[1], Kyunghoon Lee[1], Grant Leum[1], Kongyi Li[1], Tyler Lindemann[1], Matthew Looij[1], Julie Love[1], Marijn Lucas[1], Roman Lutchyn[1], Morten Hannibal Madsen[1], Nash Madulid[1], Albert Malmros[1], Michael Manfra[1], Devashish Mantri[1], Signe Brynold Markussen[1], Esteban Martinez[1], Marco Mattila[1], Robert McNeil[1], Antonio B. Mei[1], Ryan V. Mishmash[1], Gopakumar Mohandas[1], Christian Mollgaard[1], Trevor Morgan[1], George Moussa[1], Chetan Nayak[1]✉, Jens Hedegaard Nielsen[1], Jens Munk Nielsen[1], William Hvidtfelt Padkær Nielsen[1], Bas Nijholt[1], Mike Nystrom[1], Eoin O'Farrell[1], Thomas Ohki[1], Keita Otani[1], Brian Paquelet Wütz[1], Sebastian Pauka[1], Karl Petersson[1], Luca Petit[1], Dima Pikulin[1], Guen Prawiroatmodjo[1], Frank Preiss[1], Eduardo Puchol Morejon[1], Mohana Rajpalke[1], Craig Ranta[1], Katrine Rasmussen[1], David Razmadze[1], Outi Reentila[1], David J. Reilly[1], Yuan Ren[1], Ken Reneris[1], Richard Rouse[1], Ivan Sadovskyy[1], Lauri Sainiemi[1], Irene Sanlorenzo[1], Emma Schmidgall[1], Cristina Sfiligoj[1], Mustafeez Bashir Shah[1], Kevin Simoes[1], Shilpi Singh[1], Sarat Sinha[1], Thomas Soerensen[1], Patrick Sohr[1], Tomas Stankevic[1], Lieuwe Stek[1], Eric Stuppard[1], Henri Suominen[1], Judith Suter[1], Sam Teicher[1], Nivetha Thiyagarajah[1], Raj Tholapi[1], Mason Thomas[1], Emily Toomey[1], Josh Tracy[1], Michelle Turley[1], Shivendra Upadhyay[1], Ivan Urban[1], Kevin Van Hoogdalem[1], David J. Van Woerkom[1], Dmitrii V. Viazmitinov[1], Dominik Vogel[1], John Watson[1], Alex Webster[1], Joseph Weston[1], Georg W. Winkler[1], Di Xu[1], Chung Kai Yang[1], Emrah Yucelen[1], Roland Zeisel[1], Guoji Zheng[1] & Justin Zilke[1]

[1]Microsoft Quantum, Redmond, WA, USA. ✉e-mail: cnayak@microsoft.com